NAVAL POSTGRADUATE SCHOOL

MONTEREY, CALIFORNIA

THESIS

HORIZONTAL NEARSHORE SURFACE DISPERSION FOR THE FLORIDA PANHANDLE

by

Kate J. Woodall

June 2014

Thesis Advisor:	James MacMahan
Second Reader:	Edward Thornton

Approved for public release; distribution is unlimited

THIS PAGE INTENTIONALLY LEFT BLANK

REPORT DOCUMENTATION PAGE

Form Approved OMB No. 0704–0188

1. AGENCY USE ONLY *(Leave blank)*	**2. REPORT DATE** June 2014	**3. REPORT TYPE AND DATES COVERED** Master's Thesis

4. TITLE AND SUBTITLE
HORIZONTAL NEARSHORE SURFACE DISPERSION FOR THE FLORIDA PANHANDLE

5. FUNDING NUMBERS

6. AUTHOR(S) Kate J Woodall

7. PERFORMING ORGANIZATION NAME(S) AND ADDRESS(ES)
Naval Postgraduate School
Monterey, CA 93943-5000

8. PERFORMING ORGANIZATION REPORT NUMBER

9. SPONSORING /MONITORING AGENCY NAME(S) AND ADDRESS(ES)
N/A

10. SPONSORING/MONITORING AGENCY REPORT NUMBER

11. SUPPLEMENTARY NOTES The views expressed in this thesis are those of the author and do not reflect the official policy or position of the Department of Defense or the U.S. Government. IRB Protocol number ____N/A____.

12a. DISTRIBUTION / AVAILABILITY STATEMENT
Approved for public release; distribution is unlimited

12b. DISTRIBUTION CODE

13. ABSTRACT (maximum 200 words)

Knowledge of how a buoyant tracer is horizontally dispersed in the nearshore environment is important for a variety of applications, from aiding oil-spill cleanup strategies to detecting drifting mines. Horizontal nearshore surface dispersion for the Florida panhandle was investigated using 75 drifters deployed over a five-day period during the Surfzone Coastal Oil Pathways Experiment (SCOPE) in December 2013. The data set consisted of 382 original drifter pairs in the spatial range of ~ 5 m to ~ 4.5 km with drifter position sampled every 1 sec for a duration of ~ 30 – 40 hours.

Lagrangian flow descriptions revealed that the drifters moved coherently with the majority of drifter trajectories correlated with the surface current forced by the local wind field. The horizontal dispersion estimate was quantified using two-particle statistics, D^2, and Finite Scale Lyapunov Exponent, λ, methodologies. D^2 results revealed a generally ballistic, $D^2 \sim t^2$, path-followed regime, with λ results exhibiting enhanced growth over scales < 100 m, with Richardson like growth, $\lambda \sim \delta^{-2/3}$, for scales > 100 m. It is conjectured that the mechanisms responsible for influencing the horizontal nearshore surface dispersion for the Florida panhandle are complex and likely a combination of mechanisms from small-scale coherent motions to shear, but predominately being forced by the surface current induced by the local wind field. Variability in D^2 values is attributed to the orientation change of the drifter trajectories coupled with the variability in the wind field.

14. SUBJECT TERMS Horizontal dispersion, relative dispersion, diffusivity, Beasley Park, drifters, Lagrangian, ADCP.	**15. NUMBER OF PAGES** 55
	16. PRICE CODE

17. SECURITY CLASSIFICATION OF REPORT	**18. SECURITY CLASSIFICATION OF THIS PAGE**	**19. SECURITY CLASSIFICATION OF ABSTRACT**	**20. LIMITATION OF ABSTRACT**
Unclassified	Unclassified	Unclassified	UU

NSN 7540–01-280-5500

Standard Form 298 (Rev. 2–89)
Prescribed by ANSI Std. 239–18

THIS PAGE INTENTIONALLY LEFT BLANK

Approved for public release; distribution is unlimited

HORIZONTAL NEARSHORE SURFACE DISPERSION FOR THE FLORIDA PANHANDLE

Kate J. Woodall
Lieutenant Commander, Royal Australian Navy
B.S., University of New South Wales at Australian Defence Force Academy, 2004

Submitted in partial fulfillment of the
requirements for the degree of

MASTER OF SCIENCE IN PHYSICAL OCEANOGRAPHY

from the

NAVAL POSTGRADUATE SCHOOL
June 2014

Author: Kate J. Woodall

Approved by: James MacMahan, Ph.D.
Thesis Advisor

Edward Thornton, Ph.D.
Second Reader

Peter Chu, Ph.D.
Chair, Department of Oceanography

THIS PAGE INTENTIONALLY LEFT BLANK

ABSTRACT

Knowledge of how a buoyant tracer is horizontally dispersed in the nearshore environment is important for a variety of applications, from aiding oil-spill cleanup strategies to detecting drifting mines. Horizontal nearshore surface dispersion for the Florida panhandle was investigated using 75 drifters deployed over a five-day period during the Surfzone Coastal Oil Pathways Experiment (SCOPE) in December 2013. The data set consisted of 382 original drifter pairs in the spatial range of ~ 5 m to ~ 4.5 km with drifter position sampled every 1 sec for a duration of ~ 30 – 40 hours.

Lagrangian flow descriptions revealed that the drifters moved coherently with the majority of drifter trajectories correlated with the surface current forced by the local wind field. The horizontal dispersion estimate was quantified using two-particle statistics, D^2, and Finite Scale Lyapunov Exponent, λ, methodologies. D^2 results revealed a generally ballistic, $D^2 \sim t^2$, path-followed regime, with λ results exhibiting enhanced growth over scales < 100 m, with Richardson like growth, $\lambda \sim \delta^{-2/3}$, for scales > 100 m. It is conjectured that the mechanisms responsible for influencing the horizontal nearshore surface dispersion for the Florida panhandle are complex and likely a combination of mechanisms from small-scale coherent motions to shear, but predominately being forced by the surface current induced by the local wind field. Variability in D^2 values is attributed to the orientation change of the drifter trajectories coupled with the variability in the wind field.

THIS PAGE INTENTIONALLY LEFT BLANK

TABLE OF CONTENTS

THIS PAGE INTENTIONALLY LEFT BLANK

LIST OF FIGURES

LIST OF ACRONYMS AND ABBREVIATIONS

ADCP	acoustic Doppler current profiler
CARTHE	Consortium for Advanced Research on Transport of Hydrocarbon in the Environment
CO-OPS	Center for Operational Oceanographic Products and Services
CTD	conductivity, temperature, depth instrument
CSTARS	Centre for Southeastern Tropical Advanced Remote Sensing
FIU	Florida International University
FSLE	Finite Scale Lyapunov Exponent
GPS	Global Positioning System
LED	light emitting diode
LC	Langmuir circulation
LST	local standard time
NOAA	National Oceanic and Atmospheric Administration
NOS	National Ocean Service
PVC	polyvinyl chloride
RSMAS	Rosenstiel School of Marine and Atmospheric Science
SCOPE	Surfzone Coastal Oil Pathways Experiment
UM	University of Miami

THIS PAGE INTENTIONALLY LEFT BLANK

ACKNOWLEDGMENTS

I would like to thank my thesis advisor, Jamie MacMahan, for his outstanding support, thirst for knowledge and ability to involve his students in the process of scientific research. I also thank Jamie MacMahan and Jenna Brown, who provided data-processing assistance, and my brother Nathan Stevenson, who helped me tirelessly with MATLAB. To all those involved with the Surfzone Coastal Oil Pathways Experiment (SCOPE), who were instrumental in the acquisition of data used in this research, thank you. Thanks to my husband, Robert Woodall, and parents, Russell and Linda Stevenson, for their continual support and inspiration throughout this entire process.

THIS PAGE INTENTIONALLY LEFT BLANK

I. INTRODUCTION

A. BACKGROUND

The *Deepwater Horizon* oil-drilling rig explosion, off the coast of Louisiana in the Gulf of Mexico on 20 April 2010, that caused 11 fatalities, released an estimated total of more than 200 million U.S. gallons of crude oil into the ocean environment (Ramseur et al. 2013). Response efforts in the days succeeding the explosion were largely targeted at preventing the oil from reaching the shorelines of the Gulf States; however, the oil did eventually contaminate hundreds of miles of shoreline (Ramseur et al. 2013). Understanding how this oil, a buoyant tracer, is transported in the surface layer of the ocean and reaches the shore to the extent of that seen during the *Deepwater Horizon* spill is critical to aid oil-spill mitigation strategies for the future. This understanding of material transport in the surface layer has other important applications, from the search and rescue of personnel or high-value objects, the tracking of drifting mines to biological or temperature distributions (Özgökmen and Griffa 2011). Material transport in the nearshore, defined in this research as the inner shelf region seaward of the surfzone to a few kilometers, is not well understood and is the focus of this research.

B. THE STUDY OF MATERIAL TRANSPORT

The transport of a buoyant tracer can simply be considered by its advection and dispersion collapsing the complexity of the ocean into these two terms (Drake and Edwards 2009). "Advection" is defined by the mean flow. "Dispersion" considered herein is the horizontal mixing of particles associated with variable aspects of the flow, such as turbulence, shear, and small-scale coherent motions (Schroeder et al. 2011). Dispersion quantifies horizontal mixing, but also provides a description of dynamical scale as a function of time, i.e., its evolution (Schroeder et al. 2011). A realistic evaluation of the dispersion requires a Lagrangian description, whereby particle motions within the flow field are continuously observed (Moroni et al. 2002). Dispersion can be determined through either field observations, using drifter trajectories or tracer releases, or through numerical modeling simulations of particle trajectories, the latter of which is

becoming more popular in current research initiatives (e.g., Romero et al. 2013; Schroeder at al. 2012; Schroeder et al. 2011; Haza et al. 2010; Poje et al. 2010).

The ocean environment is inherently highly variable, causing individual particle trajectories to behave unpredictably; as a result, the measure of dispersion requires a statistical description to account for this variability (LaCasce 2008). It should be noted that the statistical approach assumes homogeneity and stationarity, both of which cannot be equivocally assumed for the ocean (Davis 1991). Two classic statistical measures of dispersion are Taylor (1921) absolute dispersion theory and Richardson (1926) relative dispersion theory. Absolute dispersion (σ^2) quantifies how a single particle is advected from a common release point over many releases (Spydell et al. 2007), and characterizes dispersion influenced by the larger scales of the flow (Romero et al. 2013). Relative dispersion (D^2) measures the changes in the separation of particles relative to each other (mean particle pair separation), about the center of mass (Brown et al. 2009) and characterizes the dispersion influenced by the smaller scale features of the flow (Lumpkin et al. 2010). The rate of change of dispersion over time is termed its *diffusivity* and again there are two measures of diffusivity; the measure derived from the absolute dispersion, the absolute diffusivity (κ), and that derived from relative dispersion, the relative diffusivity (μ).

This research focuses on examining the relative horizontal dispersion in the surface layer of the ocean that is commonly computed through the mean square particle pair separation as briefly described above, and described in more detail in Chapter III. However, an alternative approach that is also considered, and described in more detail in Chapter III, considers the Finite Scale Lyapunov exponent (FSLE) (e.g. Romero et al. 2013; Schroeder et al. 2012; Haza et al. 2010; Poje et al. 2010). This metric considers distance as the independent variable and averages particle pair separations instead over time, which solves the problems encountered when averaging drifter pairs with differing separation distances (LaCasce 2008).

After the horizontal dispersion for a region of interest has been quantified through either metric as described above, the mechanism or mechanisms responsible for

influencing its evolution need to be considered. As a means to determine this mechanism, the literature predominately discusses ascertaining whether an area is experiencing local or non-local dispersion. Local dispersion indicates the horizontal dispersion is controlled by eddies comparable in scale to the separation distance between particle pairs and corresponds to sub-mesoscale features of the flow (Schroeder et al. 2013). Non-local dispersion is instead controlled by eddies larger in scale than the separation distance between particle pairs and corresponds to mesoscale features of the flow (Schroeder et al. 2012). How the dispersion grows in time correlates to different dispersion regimes that subsequently correspond to either local or non-local dispersion. If the dispersion grows exponentially in time, $D^2 \sim \exp(t)$, then the dispersion is non-local. If the dispersion does not exhibit exponential growth it suggests a power-law dependence in time and grows as either, diffusive (random) $D^2 \sim t$, ballistic/Batchelor (path-followed) $D^2 \sim t^2$ or Richardson $D^2 \sim t^3$, which corresponds to local dispersion (Richardson 1926; Batchelor 1950; LaCasce and Ohlmann 2003; LaCasce 2008; Koszalka et al. 2009; Lumpkin and Elipot 2010; Haza et al. 2010; Schroeder et al. 2012; Romero et al. 2013). It should be noted however, that these dispersion growth regimes were mostly developed on a theoretical basis and are intrinsically linked to turbulence cascade theory (Haza et al. 2008). The extent, to which these classical regimes are actually realized in the ocean environment, is varied and may not have a clear fit in explaining the horizontal dispersion observed in the complex nearshore region.

C. PREVIOUS RESEARCH

Fundamental research on ocean dispersion has focused either on absolute dispersion due to the absence of close enough particle pairs or relative dispersion using so called “chance pairs.” More recently, over the last decade, studies on relative dispersion using targeted drifter pair deployments have been made with surface or sub-surface drifters and reveal large inconsistencies for predicted dispersive regimes. The majority of these studies examine dispersion for the open ocean environment with initial drifter pair separations on the order of 10km (e.g., LaCasce and Bower 2000; LaCasce and Ohlmann 2003; Kozalka et al. 2009; Lumpkin et al. 2010; Haza et al. 2010; Schroeder et al. 2011), with a few studies focusing on dispersion in the surfzone region (e.g., Spydell et al. 2007;

Spydell et al. 2009; Brown et al. 2009). Research in the nearshore environment outside of the surfzone involves complex coastal dynamics, and is arguably a more important area for research due to environmental problems in this region having increased societal implications. Only a few recent studies have been performed describing the dispersion for the inner shelf region (e.g. Romero et al. 2013; Schroeder et al. 2012; Ohlmann et al. 2012).

In the open ocean LaCasce and Bower (2000) in their study of subsurface floats in the North Atlantic, found results that varied from diffusive, $D^2 \sim t$, to Richardson-like, $D^2 \sim t^3$, for separations of 10 km to 100–200 km. LaCasce and Ohlmann (2003), in their study of pairs and triplets of surface drifters in the Gulf of Mexico, found exponential growth, $D^2 \sim \exp(t)$, for scales ~ 1 km to 40–50 km initially, followed by a power law dependence for larger scales suggesting a roughly ballistic regime, $D^2 \sim t^2$, in the late period. Kozalka et al. (2009) examined surface drifters deployed in the Nordic Seas, they found that in the first few days, for spatial scales of less than 10 km an exponential regime, $D^2 \sim \exp(t)$, was observed, then from 2 to 10 days and scales 10 – 100 km the relative dispersion displayed a Richardson regime, $D^2 \sim t^3$, and then became diffusive, $D^2 \sim t$, in the late period and with greater scales. Lumpkin et al. (2010) examined surface drifter pairs deployed in the Gulf Stream region; their results found a Richardson like, $D^2 \sim t^3$, behavior of dispersion for scales 1–3 km to 300–500km. Haza et al. (2010) examined the transport characteristics in the Gulf of La Spezia on the western coast of Italy using surface drifters, and found an exponential relative dispersion regime, $D^2 \sim \exp(t)$. Schroeder et al. (2011) studied relative dispersion in the Liguro-Provençal basin using clusters of drifters over a two-year period and, their results indicated a clear exponential, $D^2 \sim \exp(t)$, behavior for scales ~ 1 km to 10 – 20 km.

In the surfzone environment, Spydell et al. (2007) using drifter observations within 200 m of the shoreline on a sandy beach in San Diego, California, found relative dispersion that differed from the classical regimes with growth like, $D^2 \sim t^{3/2}$. Brown et al. (2009) examined surf zone drifters at Sand City, Monterey Bay, California, and also found growth that differed from the classical regimes like, $D^2 \sim t^{4/3}$.

The recent limited studies in the nearshore environment examined the relative dispersion over the sub-mesoscale range, on the order of 1 km. Schroeder et al. (2012) observed relative dispersion in the North-Western Mediterranean Sea and targeted the sub-mesoscale range of 100 m to 1 km, and characterized the dispersion over this scale as initially enhanced during the first ~15 hours followed by a second regime that was characterized by slower growth for the following days. For scales greater than ~ 10 km a ballistic growth, $D^2 \sim t^2$, was observed. From clusters of surface drifters in the Santa Barbara channel Ohlmann et al. (2012) observed exponential growth, $D^2 \sim \exp(t)$, for smaller separation scales ~ 5 to 100 m over the first ~ 5 hours followed by a ballistic regime, $D^2 \sim t^2$, with scales between 100m and 1 km. Romero et al. (2013) examined relative dispersion by numerical simulations of particle trajectories generated for Southern California, using Regional Ocean Modelling System (ROMS). Their results found monotonic growth for initial particle separations of 500 m within 15 km of the shoreline, and after ~ 12 h the growth varied between diffusive, $D^2 \sim t$, and Richardson like, $D^2 \sim t^3$.

It appears from the literature that open ocean relative dispersion estimates follow more closely with classical theoretical dispersion regimes than estimates in the surfzone and nearshore regions, which may require additional considerations to explain the dispersion in this complex environment. Therefore, in considering the mechanism responsible for horizontal dispersion in the nearshore area, dynamics other than turbulent processes need to be considered to ensure a robust assessment is made.

D. THESIS OBJECTIVES

My thesis research aims to determine the horizontal nearshore surface dispersion regime in the vicinity of Beasley Park, Okaloosa Island, Florida, and aims to describe the mechanisms that are influencing its evolution. This study examines horizontal nearshore surface dispersion through two-particle statistic and FSLE methodologies for the Florida panhandle using data sets obtained from drifter deployments during the Surf Zone Coastal Oil Pathways Experiment (SCOPE), during December 2013. This thesis is organized as follows. Chapter II provides a description on the experiment, area of

interest, deployment scheme and drifter data. Chapter III discusses the mathematical background and in Chapter IV, results are provided. The results are discussed in Chapter V and a summary is given in Chapter VI that includes a conclusion and recommendations for future research.

II. EXPERIMENT

A. AREA OF INTEREST

The study area was offshore of the surf zone in the vicinity of Beasley Park, Okaloosa Island, Florida (Fig. 1). The area was characterized by depths around 20 m and was influenced by the Choctawhatchee River and Bay watershed discharge from the Destin Inlet also referred to as East Pass. Prior to the field experiment, considerations for an appropriate sampling strategy were made to ensure the reliability of the relative dispersion results and to resolve differing scales of motion. The drifter deployment strategy consisted of seven positions where drifters were deployed: four positions in the cross-shore extending to 4.5 km offshore, where three drifters (triplets) were deployed simultaneously, and another three positions to the east of the cross-shore of the four triplet positions, where a single drifter was released. This allowed for four small triangle areas and three large triangle areas to aid in resolving the differing scales of motion influencing the relative dispersion from just outside the surfzone to 4.5 km offshore for this area (Fig. 1).

Other instrumentation included a conductivity, temperature and depth (CTD) gauge, which was cast prior to each drifter release to measure in situ salinity data to aid in the identification of the buoyant coastal front location as it exited the Destin Inlet. An acoustic Doppler current profiler (ADCP) deployed in 10 m of water in the vicinity of the 0.5 km drifter release position, Figure 1, to measure the vertical velocity structure every 1 sec for the duration of SCOPE. And a meteorological instrumented 10 m tower installed in the John Beasley Park car park, Figure 1, to measure the u and v velocity components of the wind field, from the International Hurricane Research Center, FIU. The data obtained from these instruments were evaluated and are discussed below.

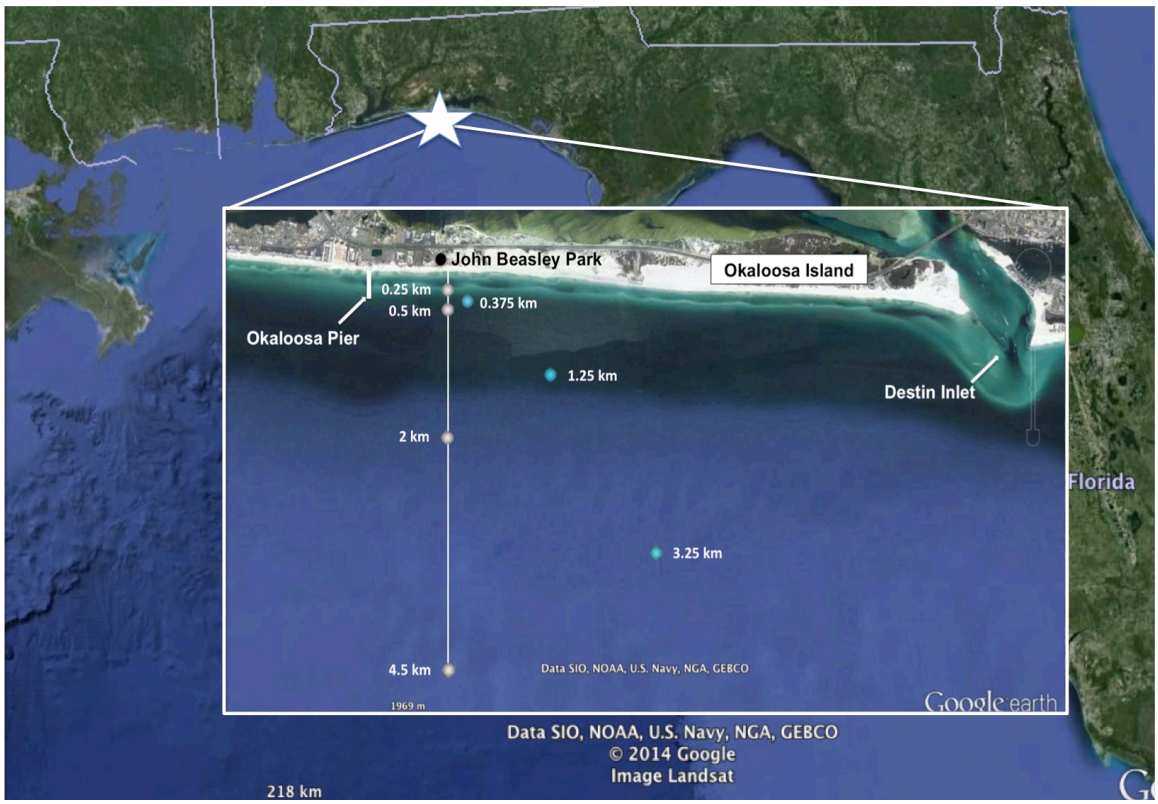

Figure 1. The Surfzone Coastal Oil Pathways Experiment (SCOPE) site, Beasley Park, Okaloosa Island, Florida. The inset shows the triplet release positions, 0.25 km, 0.5 km, 2 km, 4.5 km, and the single drifter release positions, 0.375 km, 3.25 km, 3.25 km, and identifies the landmarks, Okaloosa Pier, John Beasley Park and the Destin Inlet / East Pass (After Google Earth Image of experiment site 2014)

B. DRIFTER DATA

The drifters used in the five-day deployment scheme during SCOPE were designed and manufactured by Professor Jamie MacMahan and Mr. Keith Wyckoff, Naval Postgraduate School, Monterey, California, and were specifically designed for use in the coastal environment. The satellite-tracked surface drifters recorded their position every 1 sec internally using the Global Positioning System (GPS) with drifters requiring recovery to obtain the data. The drifters were composed of a 1 m high and 20 cm wide, polyvinyl chloride (PVC) pipe with caps at either end with large holes to allow water to pass freely through the drifter. One end of the PVC pipe had a five-pound weight externally attached to ensure the drifter remained upright and the other end had a 2.5 cm

Styrofoam ring around the drifter for buoyancy (Fig. 2). A GT31 GPS receiver, an light emitting diode (LED) light for recovery at night and a SPOT GPS receiver, for real time tracking (5 min update), are contained within a watertight Otter Box attached to the top of the drifter. In total, 75 drifters were deployed as per the aforementioned deployment strategy over the five-day period from 12 December 2013 through 16 December 2013, herein referred to as yeardays 346 through 350. Drifters were typically deployed between 0830 and 1200 (local time) and were released from small boats. The triplet deployments were launched one from either side off the stern and one from off the bow of an 8 m long boat in unison in an attempt to create a small triangle. Drifters were retrieved between 24 and 72 hours after deployment due to the battery life of the GT31 persisting only for approximately 48 hours.

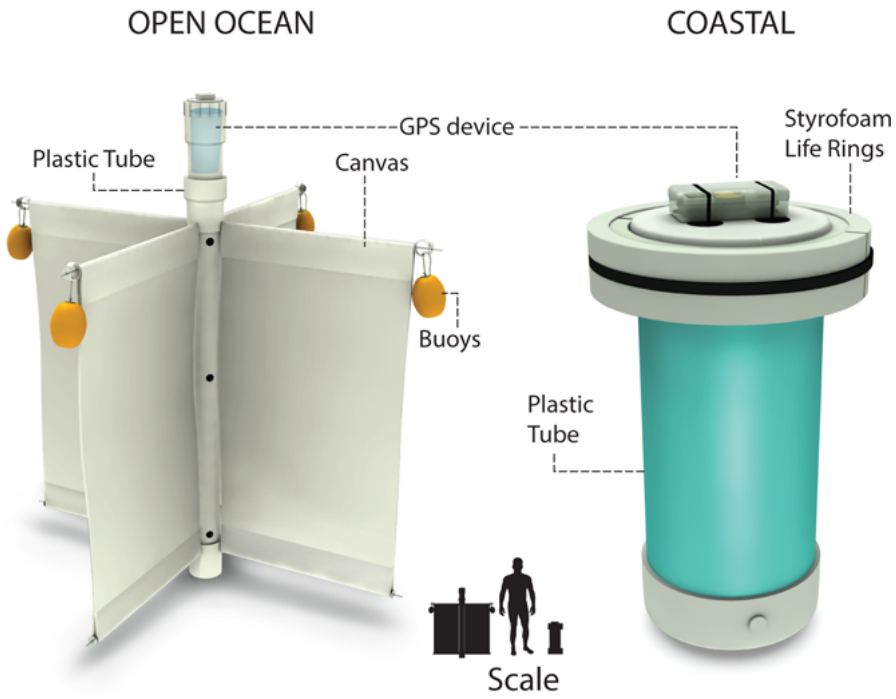

Figure 2. Schematic of the coastal drifter used during SCOPE (From CARTHE 2013).

C. ENVIRONMENTAL CONDITIONS

During the five-day drifter deployment, wave and wind conditions were variable, with wind conditions tending northerly on yearday 346 becoming easterly on yearday 347, with winds veering through south during yearday 348, becoming northerly again late on yearday 348 and persisting into yearday 349 (Fig. 3). Winds on yearday 350 were mostly north to northeasterly also veering through south to the northwest late in the day. During yearday 348 a storm event passed over the study area, by way of a frontal passage, which increased wind velocity and wave heights over the area (Fig. 3 and Fig. 4). This type of frontal passage was observed to propagate through the experiment area with a periodicity of between three to five days (Fig. 3).

The Choctawhatchee River and Bay watershed discharge from the Destin Inlet, resulted in a tidally controlled fresh water plume exiting the Destin Inlet, referred to herein as the Destin Inlet coastal buoyant front. This semi-permanent feature was a thin layer of less saline water from the surface to ~ 1 m in depth (per correspondence with Professor Brian Haus, RSMAS, UM, 2014) egressing from the Destin Inlet and observed daily, with its leading edge often observed influencing the John Beasley park experiment site during the morning period.

The differing wind and wave conditions, Figures 3 and 4, that developed from the passage of the front, in combination with the fresh water plume exiting the Destin Inlet, fed by the Choctawhatchee Bay, provided contrasting conditions for the study of nearshore surface dispersion for the area of interest.

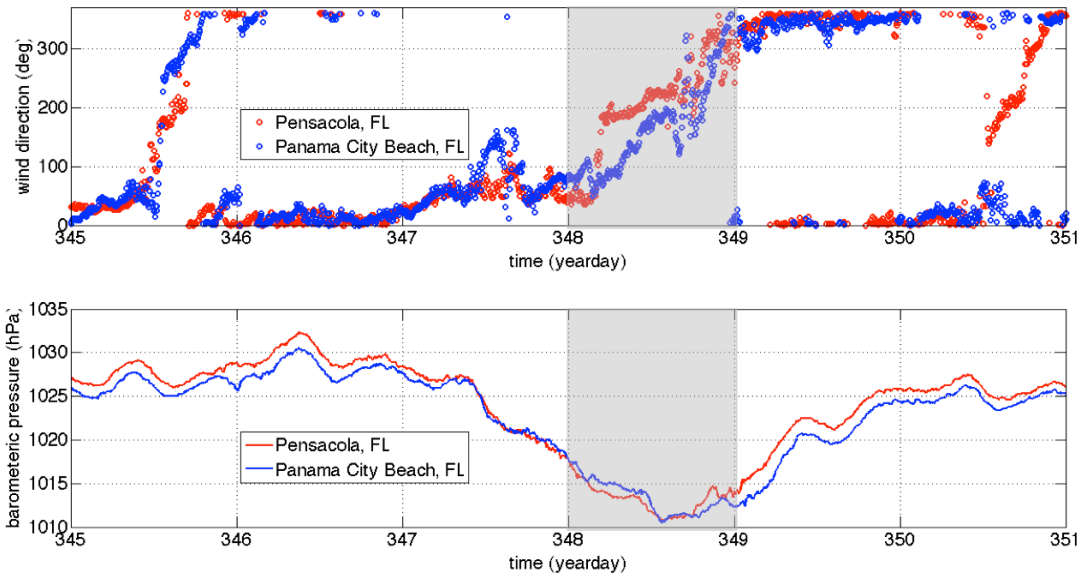

Figure 3. Upper plot, wind direction (deg) versus time (yearday) from 345 to 351 (11 through 17 December). Red dots correspond to Pensacola, FL station and blue dots, Panama City Beach, FL station. Bottom plot, barometric pressure (hPa) versus time (yearday). Red line corresponds to Pensacola, FL station and blue line, Panama City Beach, FL, station. All data from NOAA/NOS/CO-OPS. The grey shaded area in both upper and lower plots highlights the period of the frontal passage (yearday 348).

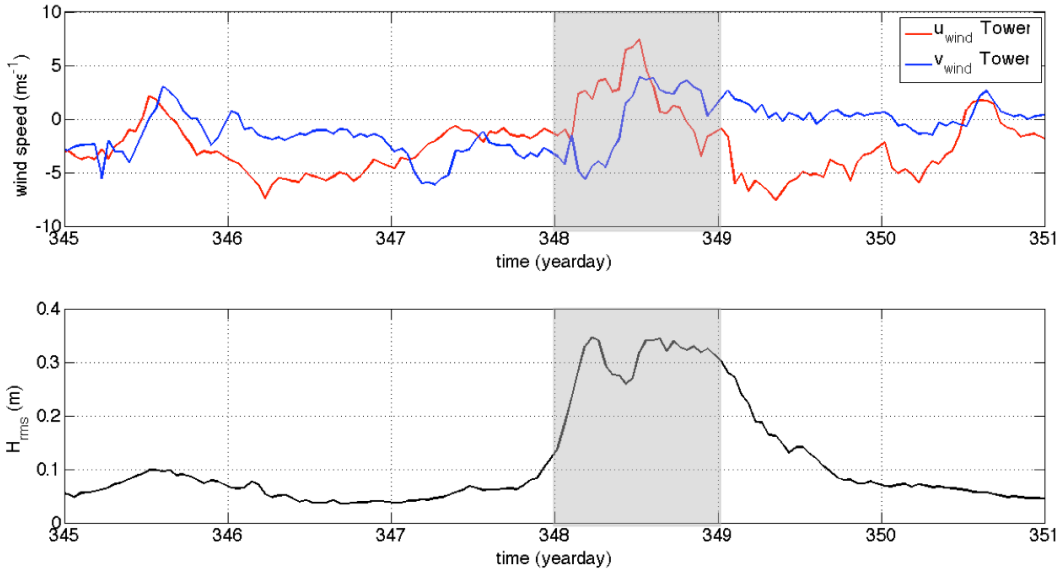

Figure 4. Upper plot, wind speed (ms^{-1}) versus time (yearday) from 345 to 351 (11 through 17 December). Red and blue lines corresponding to the u and v components, respectively, of the wind speed. Lower plot, root means square wave height, H_{rms} (m) versus time (yearday). Wind speed data are from the experiment meteorological tower on site and root mean square wave height data are derived from ADCP. The grey shaded area in both upper and lower plots highlights the period of the frontal passage (yearday 348).

III. METHODS

A. MATHEMATICAL BACKGROUND

This Chapter provides the theoretical background for the relative dispersion, relative diffusivity and FSLE estimations. First, the two-particle statistic methodology in determining relative dispersion and diffusivity are described following Spydell et al. (2007), and second the theoretical background behind the FSLE methodology is described following LaCasce (2008).

1. TWO PARTICLE STATISTICS

The Spydell et al. (2007) method describes a statistical approach to determine the mean square particle pair separation distance, D^2. In statistical terminology when considering drifter trajectories the second order moment, the variance, of the particle displacements defines the relative dispersion, which involves averaging over all particle pairs. Initially the relative separation distances between drifter pairs for each time step, $s_i(t)$, are determined, and then from these drifter pairs the relative dispersion, D_{ii}^2, the variance for all drifter separations, is calculated using

$$D_i^2(t,s_0) = \left\langle \left[s_i(t) - s_{0i} \right]^2 \right\rangle - \left\langle \left[s_i(t) - s_{0i} \right] \right\rangle^2 \tag{1.1}$$

where i = x, y; s_{0i} is the initial pair separation and the angle brackets represent ensemble averaging for all drifter pairs (Spydell et al., 2007). The relative diffusivities, μ_{ij}, the rate of change of relative dispersion is calculated using,

$$\mu_i(t,s_0) = \frac{1}{4}\frac{d}{dt} D_i^2(t,s_0) \tag{1.2}$$

where 1/4 is used instead of 1/2 because the separation of two particles is twice as large as the separation between one particle and its mean position (Brown et al., 2009).

2. FINITE SCALE LYAPUNOV EXPONENT (FSLE)

The two-particle statistic methodology described examines particle pair separations by averaging the particle pair separations over time. The FSLE is an

alternative approach to examine particle separations that instead averages over time and considers the particle pair separations as the independent variable (LaCasce 2008). LaCasce (2008) describes the relation between the FSLE to the Lyapunov exponent with its maximum reflecting the growth rate of chaotic systems. The growth rate can be determined from the Lyapunov exponent through:

$$\lambda = \lim_{t\to\infty} \lim_{y(0)\to\infty} \frac{1}{t} \ln(\overline{y(t)} / \overline{y(0)}) \tag{1.3}$$

(LaCasce 2008). To determine the FSLE, an initial distance first needs to be determined which increases by a defined factor, i.e.:

$$\delta_n = r\delta_{n-1} = r^n \delta_0 \tag{1.4}$$

where δ_0 is the initial separation distance chosen, δ_n is the multiplicatively of the initial separation distance and r is the multiplicatively factor. The time it takes, τ, for the drifter pairs to increase from one δ_n to the next multiple is recorded. The FSLE, $\lambda(\delta)$, is determined from the mean inverse of, τ, and is related to the growth rate by;

$$\lambda(\delta) = \frac{\ln(r)}{\langle \tau(\delta) \rangle} \tag{1.5}$$

The FSLE approach is useful when local dispersion regimes are influencing the flow, in that particle pair spreading is influenced by eddies of the same scale as the particle pair separations themselves (LaCasce 2008). Another benefit to its use is that all drifter pairs can be used for the calculation of FSLE no matter what the initial separation distance is, as the method averages over time instead of the separation distance (Lumpkin and Elipot 2010). One of the problems of the FSLE approach, however, is that it assumes exponential growth of the separation of drifter pairs, and from the literature there doesn't appear to be a clear agreement of how the FSLE should be calculated if the separation of drifter pairs does not grow exponentially in time (Lumpkin and Elipot 2010).

IV. RESULTS

A. LAGRANGIAN FLOW DESCRIPTIONS

Drifter trajectories over the five-day period, yearday 346 through 350, Figure 5, all behaved differently as a result of the passage of the frontal system forced by the changing synoptic conditions over the area. The drifters on yearday 346, blue line Figure 5, moved coherently offshore, before moving alongshore and finally onshore by the end of the time series. All drifters on yearday 347, green line Figure 5, moved coherently alongshore and reached the shore, influenced by the existence of a strong alongshore current. More than half of the drifters on yearday 348, red line Figure 5, reached the shore within the first ~ 5 hours, influenced by the strong onshore winds, Figures 3 and 4, with only four drifters moving offshore. Drifter trajectories on yearday 349, cyan line Figure 5, moved coherently offshore and drifters on yearday 350, magenta line, Figure 5, behaved the most erratically of all days, with their trajectories appearing to be modified by the interaction with the Destin Inlet coastal buoyant front.

The majority of drifter trajectories on each day behaved coherently, conceivably a result of the surface wind field driving the surface current. To test this hypothesis, a comparison was made between calculated surface current path lines and a single drifter trajectory for each day (Fig. 6). The current path line at the surface was obtained by integrating the upper 1 m velocity with respect to the change in time from an ADCP located in position 0.5 km, Figure 1, which crudely projects the bulk structure of the flow field in the area. This comparison shows there is a reasonable comparison between the current path line and the drifter trajectories. To determine if the surface wind field was driving the surface current a linear regression analysis between the wind and current was performed to quantify the strength of the correlation (Fig. 7). This analysis showed a slope of 0.046 (u component) and 0.076 (v component), blue and red line respectively, Figure 7, which is consistent with the literature (e.g., Hughes 1956; Smith 1968; Wu 1983). Correlation coefficients, R^2, of the data give values between 0.82 (u component) and 0.53 (v component) implying the two variables are moderately to highly correlated.

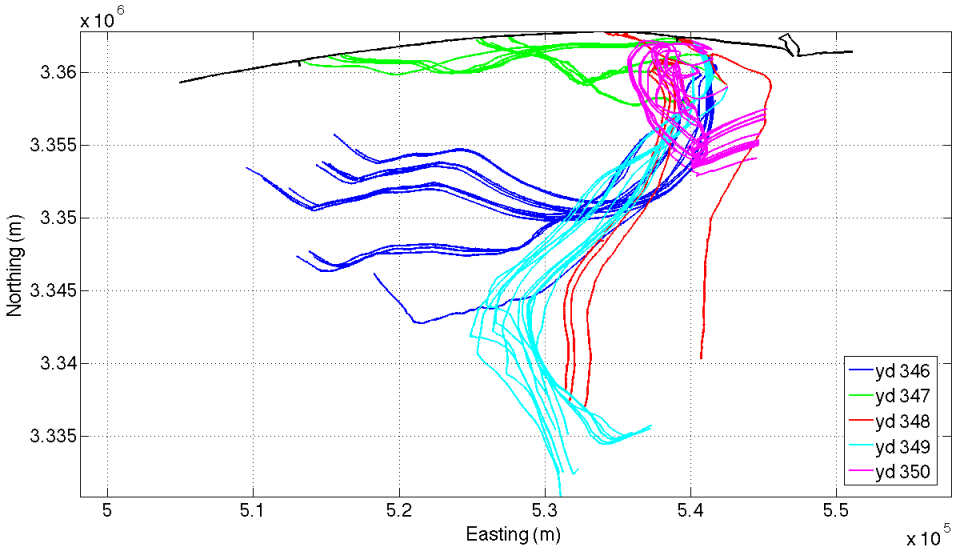

Figure 5. Drifter trajectories for drifters deployed over the five-day period, yearday 346 through 350. The colours represent the different drifter deployment yeardays as per the legend.

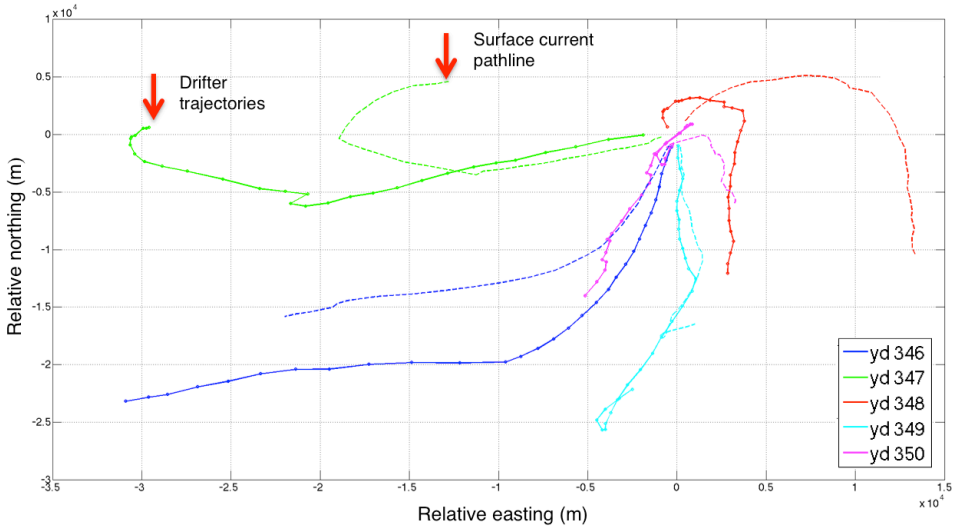

Figure 6. Surface current path line versus drifter trajectory, taken from the ADCP located nearest to the 0.5 km drifter release position. Coloured by sampling yearday with the dashed line (--) representing the calculated surface current path line (as well as indicated by the red arrow and text) and the sold line (–) representing a single drifter trajectory taken from the 0.5 km drifter deployment position.

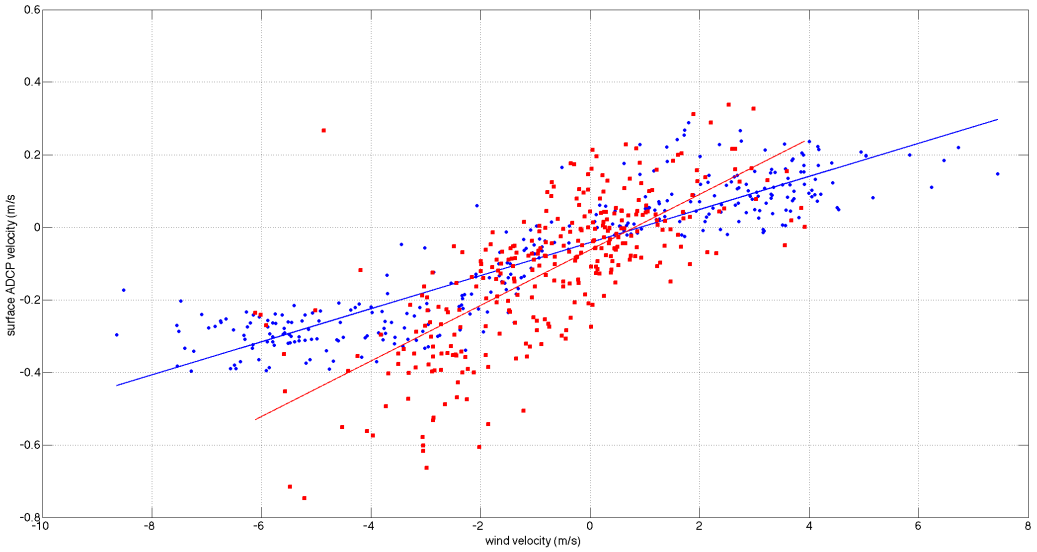

Figure 7. Linear regression of surface wind velocity (ms^{-1}) versus upper 1 m current velocity (ms^{-1}). The blue squares represent the u velocity component and the red squares represent the v velocity component, with the blue and red lines representing the line of best fit of the u (blue line) and v (red line) components between the wind and surface current field data.

Next, the proximity of the drifters to the Destin Inlet coastal buoyant front is examined. On yearday 346, two drifter groups, the triplets at the 4.5 km position, red line Figure 8, and the single drifter released at the 3.25 km position, magenta dashed line Figure 8, appeared to be deployed in the Destin Inlet coastal buoyant front as determined from the surface salinity values from CTD casts conducted in each release position that indicated less saline water in both positions (Fig. 8). These drifters moved coherently together and behaved similar to the remaining groups, but potentially followed the frontal movement for a time. On yearday 348, the three drifters deployed at initial position 4.5 km, red line Figure 9, and single drifter deployed at 3.25 km, magenta dashed line Figure 9, became divergent after their initial trajectory onshore. This divergence may be attributed to the influence of the Destin Inlet coastal buoyant front as average surface salinity values obtained form CTD casts at the 3.25 km position observed slightly less saline water than the drifters released at the 4.5 km position (Fig. 9). Divergence was also observed in the drifters on yearday 350 where drifters released from the 2 km position,

blue line Figure 10, diverged from the remaining groups, and by the late period more than half of the drifters converged offshore. Both these divergent fields on yearday 350 can reasonably be attributed to the existence of the Destin Inlet coastal buoyant front as identified from remote sensing analysis from the Centre for Southeastern Tropical Advanced Remote Sensing, (CSTARS), influencing the trajectories (Fig. 10).

Overall the majority of the drifter trajectories appear correlated with the surface current forced by the surface wind, Figures 6 and 7, implying the surface flow field was relatively homogeneous for most of the drifter deployment days over the period, with several drifter trajectories on yeardays 346 and 348 and all drifters on yearday 350 modified by the influence of the Destin Inlet coastal buoyant front.

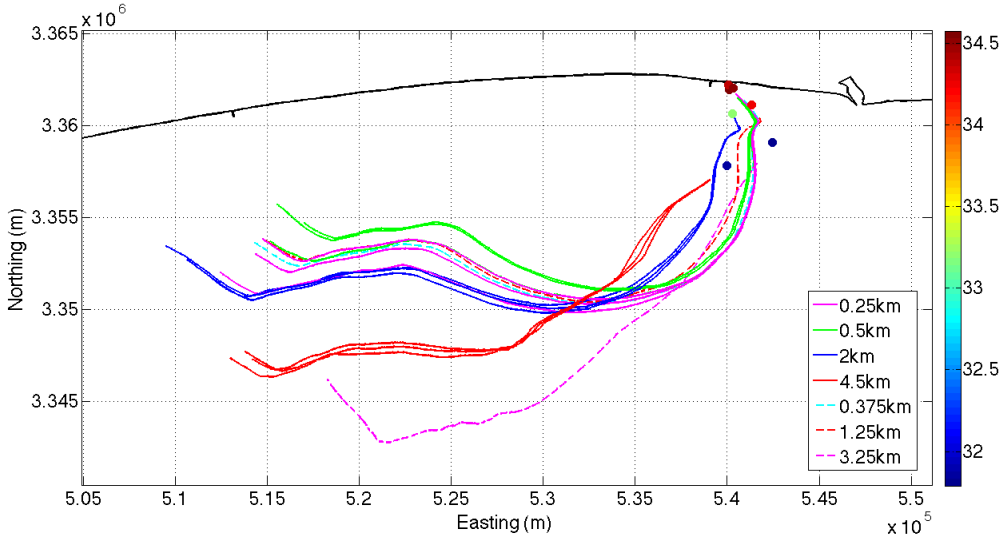

Figure 8. Drifter trajectories, yearday 346, the coloured lines represent the seven different deployment positions, from 0.25km to 4.5km. The coloured dots represent the average surface salinity for each of the seven deployment locations with the colour bar to the right of the plot representing the salinity values.

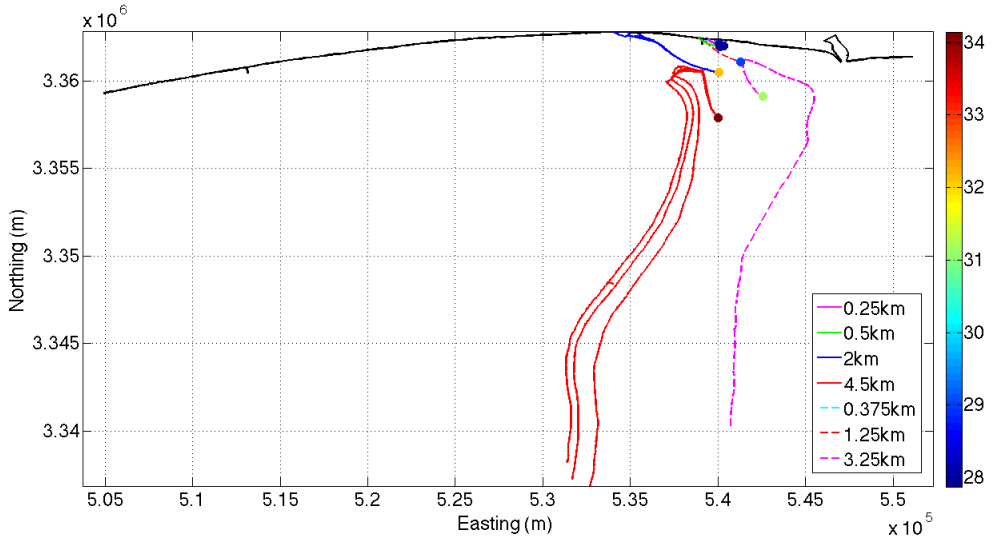

Figure 9. Same as in Figure 8, except for yearday 348.

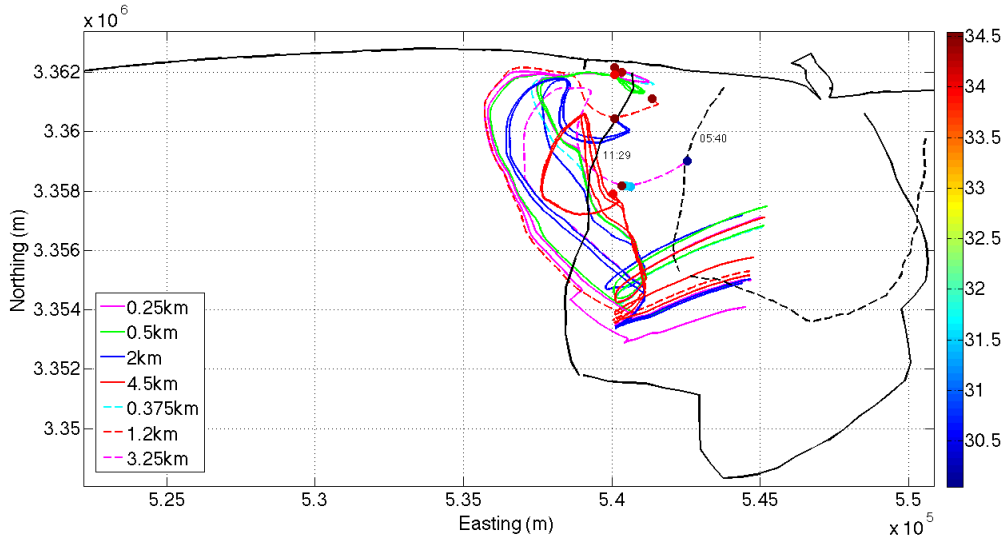

Figure 10. Same as in Figure 8, except for yearday 350. The dashed black line (--) represents the Destin Inlet coastal buoyant front location at 05:40 LST and the solid black line (–) represents the location of the front at 11:29 LST as derived from CSTARS data.

B. TWO-PARTICLE STATISTICS

From the Lagrangian flow descriptions it emerges that the drifter trajectories are influenced by the surface wind forcing the surface current for most of the days with the drifter trajectories released on yearday 346, 348 and 350, conceivably being influenced by the Destin Inlet coastal buoyant front. In estimating D^2, various combinations were considered based on the day, initial separation distance (e.g. Berti et al., 2011), and the distance the drifters were from the shoreline (e.g. Romero et al. 2013), in an attempt to fully describe the dispersion regime in the area.

Relative dispersion, D^2, was computed using Eq. (1.1) for each day of the five-day experiment (Fig. 11). The step-like appearance in Figure 11 is an artifact of the collapse in the number of drifter pairs that are available (Fig. 12). It is clear that for all days D^2 grows similarly with a period of enhanced dispersion over the first ~ 5 hours, followed by slower dispersion growth (Fig. 11). D^2 on yearday 348 behaves differently, but this may be a result of only four drifters available for the statistics as most of the drifters moved straight to the beach and were not included. Exponential growth was not observed (Fig. 11). Therefore, the dispersion is considered to be local, whereby eddies smaller in scale than the drifter pair separation are influencing the dispersion. Local dispersion suggests a power-law dependence, with D^2 following a generally ballistic regime, $D^2 \sim t^2$, with some variability outside of ~ 10 hours.

In an attempt to describe the complexity of the coastal environment, D^2 was estimated based on initial separation distances ($s_0 < 100$ m, 100 m $< s_0 <$ 2 500 m, $s_0 >$ 2 500) and drifter pair distance from the shoreline ($L_c < 1$ km, $L_c < 2$ km and $L_c > 2$ km). Similar to the daily dispersion comparison, Figure 11, these permutations all show D^2 grow with a period of enhanced dispersion over the first ~ 5 hours, followed by slower dispersion growth (Fig. 14). The power-law dependence for these permutations shows again a generally ballistic regime, $D^2 \sim t^2$ (Fig. 15).

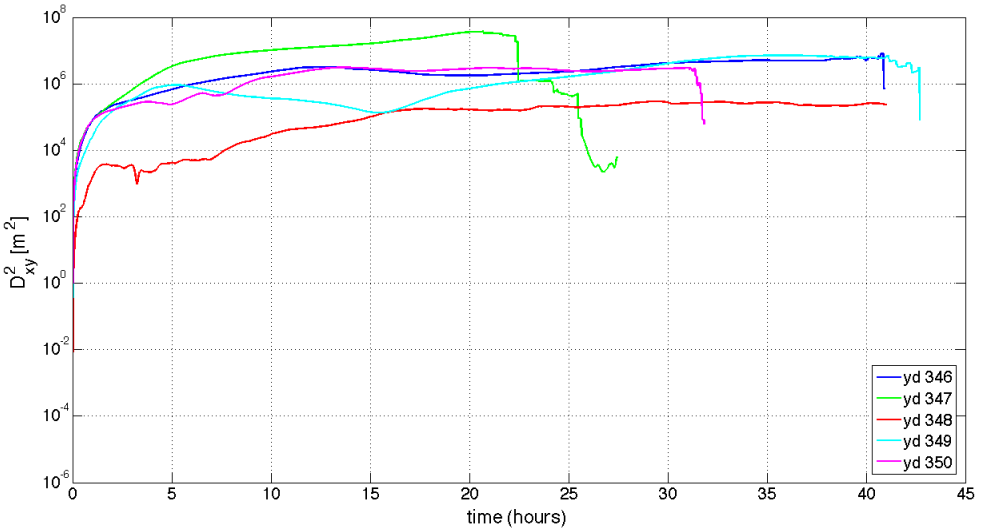

Figure 11. Semi-log plot of mean square particle pair separation distance, D^2 (m^2) versus time in hours. Coloured lines represent the different drifter deployment yeardays as per the legend.

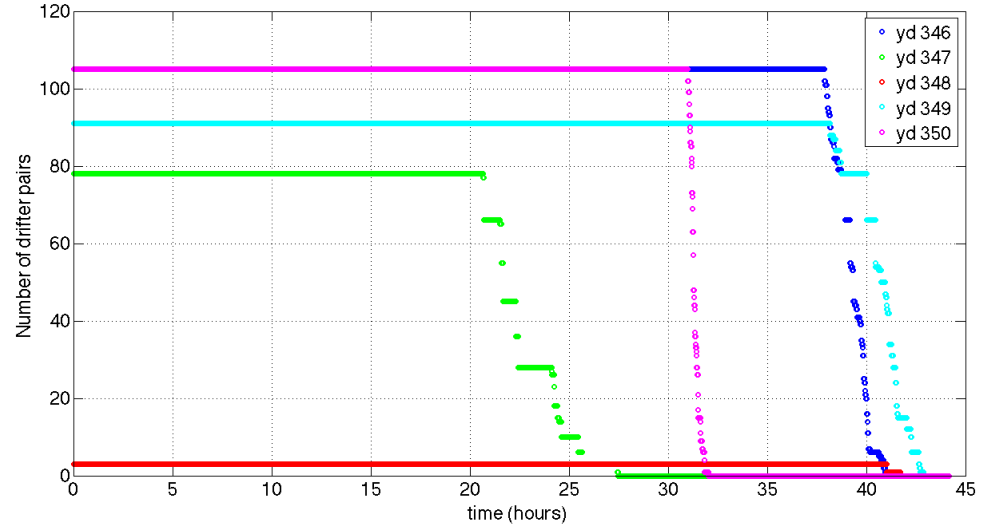

Figure 12. Number of drifter pairs versus time in hours. Coloured lines represent the different drifter deployment yeardays as per the legend.

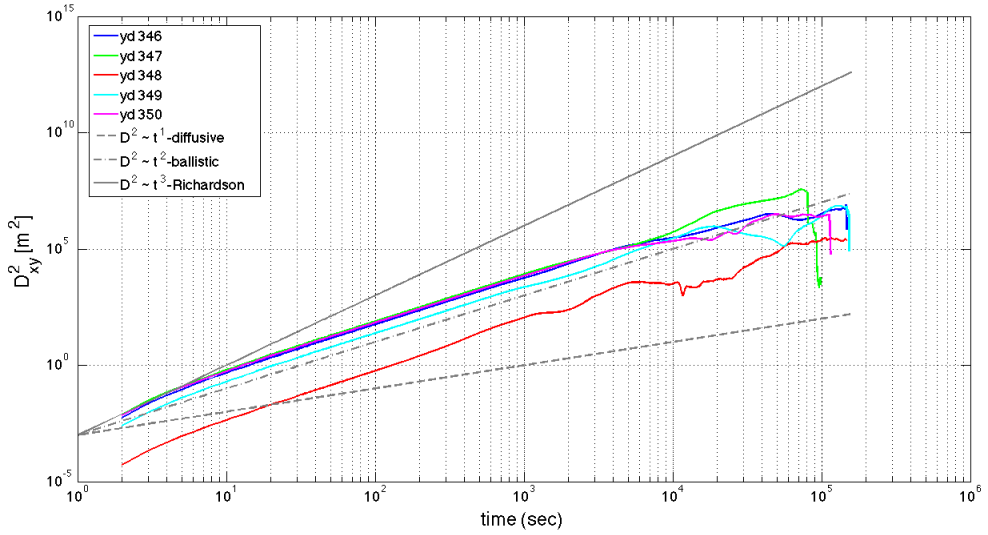

Figure 13. Log-log plot of the mean square particle pair separation distance, D^2 (m^2) versus time in seconds. Coloured lines; red, green, red, cyan and magenta represent the different drifter deployment yeardays and the grey lines represent the different dispersion growth regimes, (--) represent diffusive growth, $D^2 \sim t$, (dash dot dash) represent ballistic growth, $D^2 \sim t^2$, and (–) represent Richardson growth, $D^2 \sim t^3$.

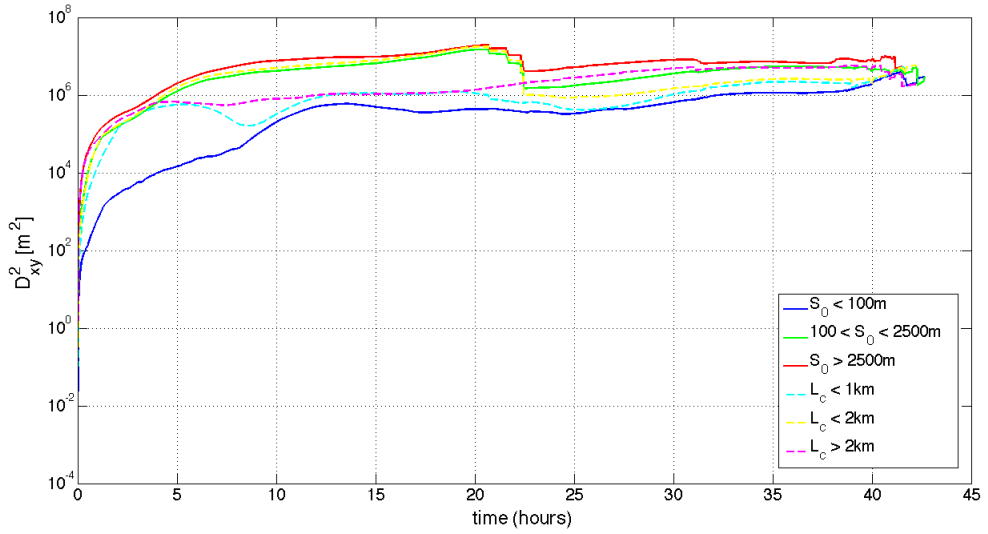

Figure 14. Same as in Figure 11 except coloured lines represent the different drifter permutations based on initial separation distance (s_0) and distance drifter pairs were from the shore.

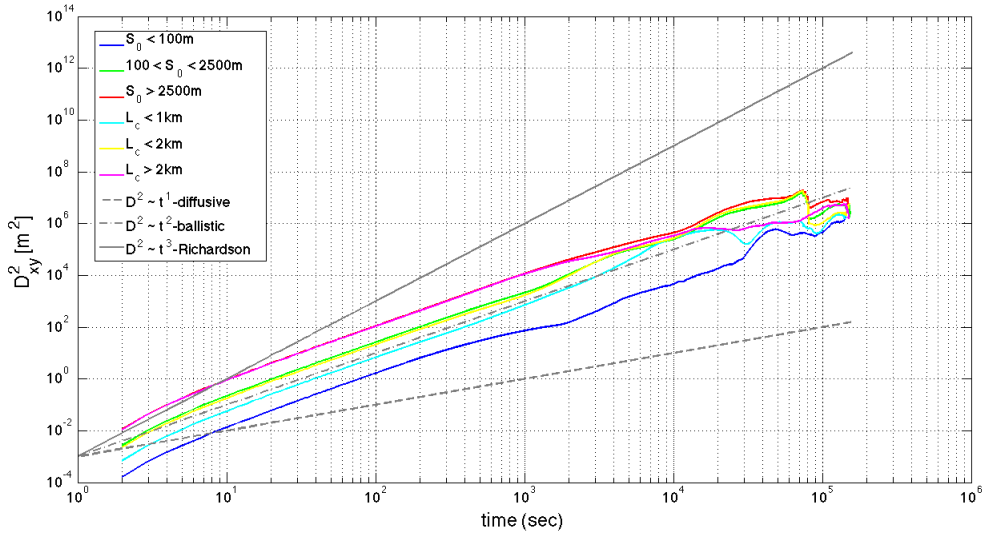

Figure 15. Same as in Figure 13, except for the coloured lines, blue, green, red, cyan, yellow and magenta represent the different drifter pair permutations based on initial separation distance (s_0) and distance drifter pairs were from the shore.

C. FINITE SCALE LYAPUNOV EXPONENT (FSLE)

The alternative approach to examine particle pair separations is computed next using the FSLE methodology (Fig. 16). The FSLE, λ, estimation is a good measure for determining the smaller scale mechanisms to dispersion. If λ is constant it is indicative of exponential growth over the scales, however, if λ is not constant across separations then it can be related to power-law growth rates. λ for each day was computed using Eq. (1.5), barring yearday 348 as most of the drifter's moved to the beach on this day and were not included. The issue of particle pair separations not increasing exponentially was managed by only using those drifter pairs that increased to all of the δ_n values selected with values for δ_0 = 10 m and r = 1.2 used in an attempt to resolve the sub-mesoscale more accurately. To note, there does need to be mathematical rigour for the FSLE calculation as it is sensitive to all types of errors as the bin sizes grow.

The FSLE results indicate a general trend for most yeardays as a Richardson like regime, $\lambda \sim \delta^{-2/3}$ for scales > 100 m with scales < 100 m showing growth faster than Richardson like but with no clear fit for any other regime. This is reasonable as the higher

λ values for the smaller scales indicates they are influenced by more turbulent systems than those of the larger scales which have a corresponding lower λ value. Yearday 350 is anomalous in the scale range > 100 m and displays an almost constant λ value. A plateau of constant λ would indicate exponential growth, which is not observed in any other yearday results and is considered to be influenced by the Destin Inlet coastal buoyant front. The remaining yeardays however support the hypothesis that local dispersion is influencing the area of interest.

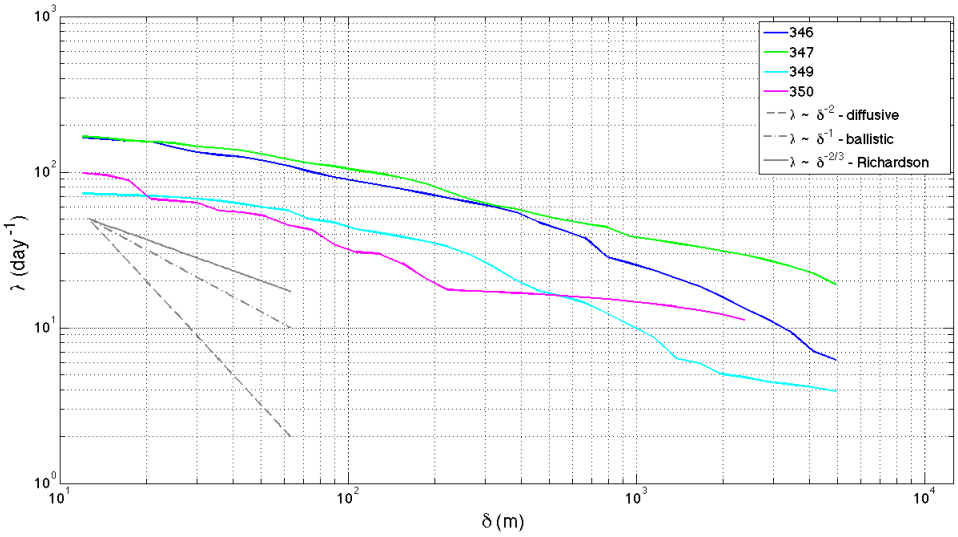

Figure 16. Log-log plot of the FSLE, λ (day^{-1}) versus separation distance, δ (m). The coloured lines, blue, green, cyan and magenta represent the different drifter yeardays, as per the legend, and the grey lines represent the different dispersion growth regimes, (--) represent diffusive growth, $\lambda \sim \delta^{-2}$, (dash dot dash) represent ballistic growth, $\lambda \sim \delta^{-1}$, and (–) represent Richardson growth, $\lambda \sim \delta^{-2/3}$.

V. DISCUSSION

The statistical confidence in the results obtained in Chapter IV are significant, implying that the interpretation of the results may lead to an understanding of what mechanisms are driving the horizontal dispersion that is occurring in the area. The results indicate that the local wind field largely influences the drifter trajectories over all days, however why this is the case is not immediately clear and requires additional conceptualization into how the wind field modifies the dispersion over time. Linear regression of the surface current with the wind field, suggests that the horizontal dispersion is influenced by fluctuations in the local surface wind field creating regions of variability in the velocity field at the ocean surface. This variability can be rapidly evolving and could illicit short-lived instabilities at the ocean surface like Langmuir circulations (LC). These LC are generated by the wind shear in combination with Stokes drift (McWilliams et al. 2000) and are aligned parallel to the wind field. The LC form within minutes of wind speeds reaching ~ 3 ms^{-1} or greater (Leibovich 1983), a threshold that is in itself variable with some LC formation observed to occur with wind speed < 3 ms^{-1} (e.g., Leibovich 1983 and McWilliams et al. 2000). These coherent instabilities are observed frequently at the ocean surface with highly variable spatial distributions (McWilliams et al. 2000). LC have previously been considered to play a role in the dispersion of material in the surface boundary layer, but predominately in the vertical extent and are not considered to be large contributors to horizontal dispersion due to their limited scales of tens of meters (McWilliams et al. 2000). The convergences and divergences observed in the drifter trajectories on yeardays 348 and 350, Figures 9 and 10, if not the consequence of the Destin Inlet coastal buoyant front, could be explained by the existence of LC.

Nerheim et al. (2006) offers an alternative mechanism induced by the wind field to LC and shows a relationship with the tracer area, or D^2, as being proportional to t^2, a relationship that in the classical theory is normally representative of ballistic growth. Nerheim et al. (2006) asserts that the t^2 dependence is a result of the wind drift depth varying in the surface layer due to changes in the wind stress and buoyancy forcing,

rather than a result of coherent eddies or sub-mesoscale dynamics. This hypothesis bears similarities to that of the LC, where vertical dispersion is predominate. However, this research utilized surface drifters, the vertical extant of which is confined to the upper one-meter of the surface layer, and variability of D^2 values over the vertical were not evaluated.

The LC and wind-drift instabilities are considered plausible mechanisms linked to the surface wind field that may influence the dispersion in the vertical scale, however, they are not intrinsically linked to horizontal dispersion. Therefore, more analysis needs to be undertaken to investigate other mechanisms that influence its evolution and variability over time. The results in Chapter IV are presented by way of log scales, Figures 11 – 14 and Figure 15, to determine the scale for D^2 which does not display the variability that is actually observed over the days. By considering the linear scale between D^2 and time, additional nuisances in the data become apparent (Fig. 17). The linear scale is more adept at describing D^2 over the entire time range due to the bias introduced in the log scale i.e., smaller values of D^2 become enhanced (Fig. 11 and 14).

In an attempt to link the surface wind field to the variability in the D^2 value, a comparison was made between D^2 over time using a scatter plot with colour representing the D^2 value, Figure 17, and with scatter plots of drifter trajectories for each day with colour again representing the D^2 value, Figure 18 through 22. It evinces from Figure 17, on yearday 346 that just before the first peak in D^2 value occurs at ~ 12 hours, D^2 values increase to a max value of $3x10^6$ (m^2) which corresponds to a change in orientation of the drifters, Figure 18. After the drifters settle on the new orientation, yearday 346, D^2 values decrease prior to an increase again before the next peak value of $5x10^6$ (m^2) at ~ 35 hours, Figure 17, which again corresponds to a change in orientation of the drifters, Figure 18. Yearday 347 experiences the same increase in D^2 values prior to a small intermediate peak at ~ 12 hours of $1.5x10^7$ (m^2), Figure 17, corresponding to a change in drifter orientation, Figure 19; however, after this intermediate peak the D^2 values continually increase to a maximum of ~ $3.5x10^7$ (m^2), Figure 17, which can be attributed to the strong alongshore current driving the shear dispersion on this day. D^2 values on yearday 348 are statistically insignificant due to the limited number of drifter pairs used for the analysis

and will not be discussed further. Yearday 349 has a small peak at ~ 5 hours that doesn't see an increase in D^2 values, Figure 17, but does have a slight corresponding change in orientation (Fig. 21). D^2 values on yearday 349 again increase prior to the secondary peak to a maximum D^2 value of $7x10^6$ at ~ 35 hours, Figure 17, which corresponds to the orientation change of the drifters (Fig. 21). Yearday 350 demonstrates variability across the first ~ 7 hours although maintaining constant D^2 values, Figure 17, which could be attributed to the influence of the Destin Inlet coastal buoyant front. D^2 values for yearday 350 then increase prior to the first major peak to a maximum D^2 value of $3x10^6$ at ~ 13 hours, Figure 17, corresponding again to an orientation change in the drifter trajectories (Fig. 22).

The variability in D^2 appears correlated with the drifter trajectory orientation change, Figure 18 through 22, with peaks in the D^2 value in Figure 17, roughly corresponding to changes in orientation for most days. The variability is not attributed to the Destin Inlet coastal buoyant front influence even though it appears to modify the Lagrangian transport of the drifters (Fig. 5). Therefore, the local wind field variability is the primary mechanism modifying the horizontal dispersion.

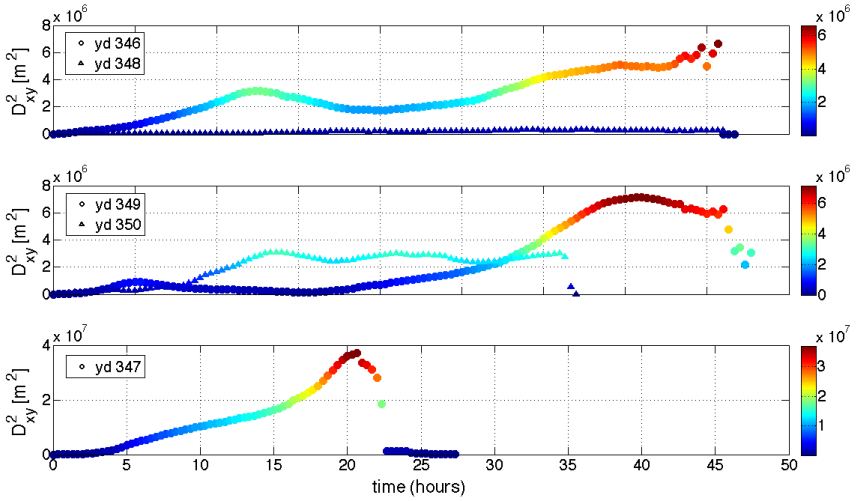

Figure 17. Scatter linear plot of mean square particle pair separation distance, D^2 (m^2) versus time in hours. Upper plot, yeardays 346 and 348, middle plot, yeardays 349 and 350 and lower plot, yearday 347. The colours represent D^2 (m^2) with the colour bar to the right of the plot representing the D^2 (m^2) values. Note the D^2 (m^2) value scale for the lower plot, yearday 347, is O(1) larger than the two other subplots.

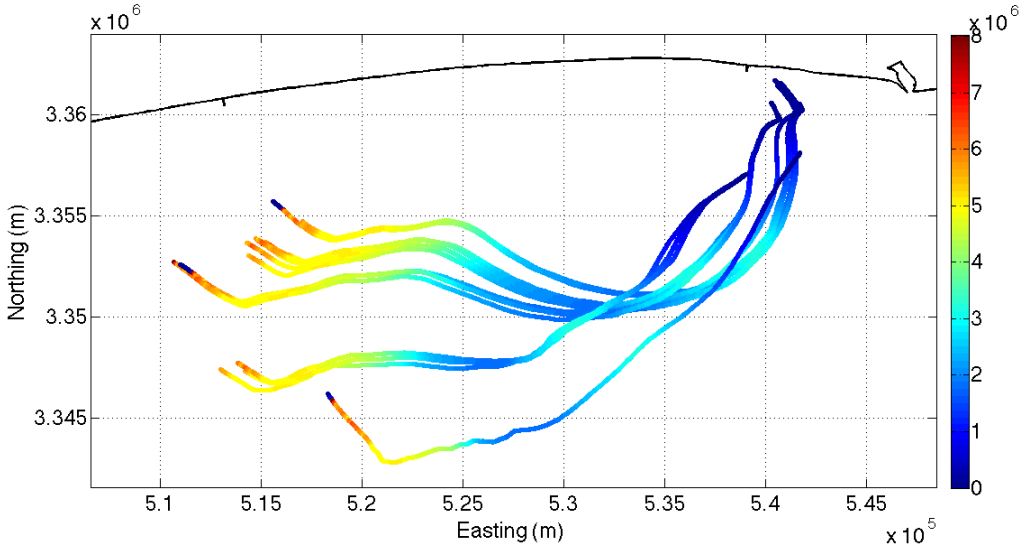

Figure 18. Scatter plot of drifter trajectories plotted on an easting and northing co-ordinate frame for yearday 346, colour represents the mean square particle pair separation distance, D^2 (m^2), with the colour bar to the right of the plot representing D^2 (m^2) values.

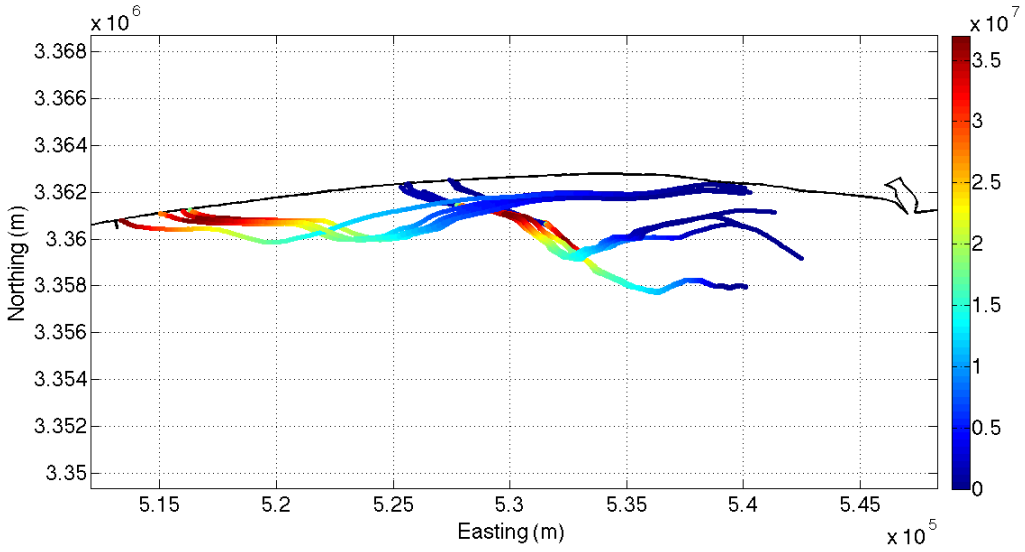

Figure 19. Same as in Figure 21 except for yearday 347.

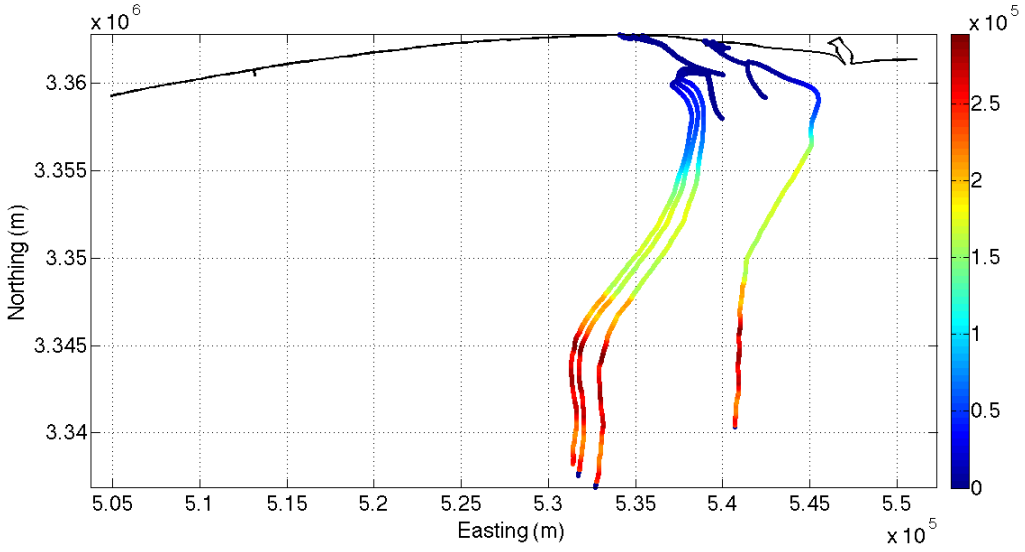

Figure 20. Same as in Figure 21 except for yearday 348.

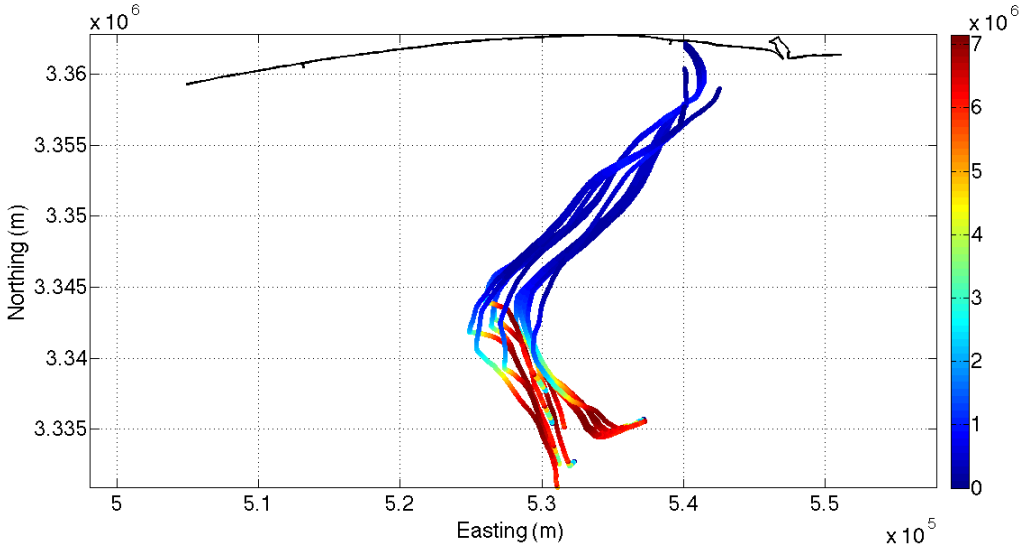

Figure 21. Same as in Figure 21 except for yearday 349.

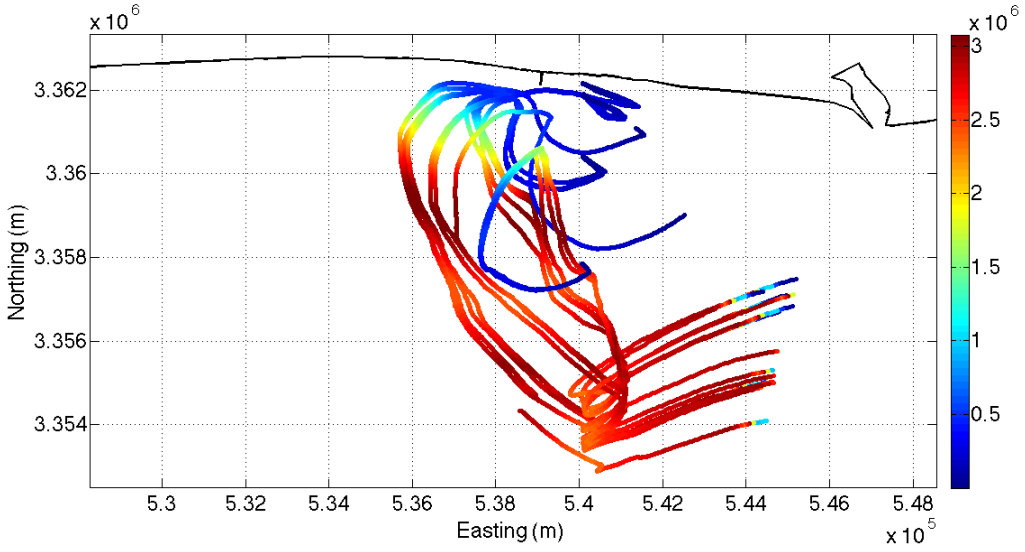

Figure 22. Same as in Figure 21 except for yearday 350.

VI. SUMMARY

A. CONCLUSION

Knowledge of horizontal surface dispersion in the nearshore region is limited, with previous research focused largely on the open ocean (e.g., LaCasce and Bower 2000; LaCasce and Ohlmann 2003; Kozalka et al. 2009; Lumpkin et al. 2010; Haza et al. 2010; Schroeder et al. 2011) and the surfzone region (e.g., Spydell et al. 2007; Spydell et al. 2009; Brown et al. 2009), with a recent shift to the nearshore region in the last few years (e.g., Romero et al. 2013; Schroeder et al. 2012; Ohlmann et al. 2012). The data reported here is unique in that no other study has obtained such a high temporal resolution over the sub-mesoscale range. From the literature, there is no clear consensus on what mechanisms influence the horizontal dispersion in the nearshore, which in turn has made it challenging to compare results with previous research, indicating that perhaps as suggested by Haza et al. (2008) dispersion in the nearshore is complex and may not be aptly relatable to classical theories.

Presented in this research are the Lagrangian flow descriptions, D^2 and FSLE results from drifter pair data collected during SCOPE. The total data set consisted of 382 drifter pairs with initial separation distances between ~5 m to ~ 4.5 km with a 1 sec sampling rate. Environmental conditions were variable over the experiment period providing juxtaposing conditions for horizontal dispersion analysis (Fig. 3 and 4). Horizontal dispersion results obtained were anomalous to those obtained for other nearshore research and were not the results that were expected. Lagrangian flow descriptions of the area revealed that most drifters behaved coherently and were found to be correlated with the surface current forced by the local wind field barring a few drifter trajectories that were modified by the influence of the Destin Inlet coastal buoyant front (Fig. 5 through 10). D^2 results revealed an initial enhanced rate followed by a slower dispersion growth, generally considered to be ballistic, t^2, indicative of shear controlling the horizontal dispersion (Fig. 11, 13 through 15). The FSLE results also exhibit enhanced growth, but over smaller scales, < 100 m, with generally Richardson like growth, t^3, for scales > 100 m (Fig. 16). The D^2 and FSLE measures are consistent in that

an exponential regime was not realized, which suggested a power law behaviour of growth that was somewhere between ballistic and Richardson. The results indicate that shear, sub-mesoscale and frontal features that are similar in scale to the drifter separations potentially drive the horizontal dispersion.

No clear fit to the classical theories for dispersion were revealed in the research which suggests that for this study area, which was found to be quasi-homogeneous and non-stationary, and at small scales, potentially other mechanisms are controlling the dispersion as suggested by Nerheim et al. (2006) and Haza et al. (2008). The inconsistent results in both methodologies and with previous research suggest that dynamics other than turbulence, shear and small-scale coherent motions may be responsible for the observed horizontal dispersion.

The proposed mechanisms influencing the horizontal dispersion in the nearshore region are ultimately considered to be more complex than observed in the open ocean. This research suggests the horizontal dispersion is predominately being forced by the local wind field driving the surface current with variability in D^2 values coupled with the wind field variability, which is altering the drifter orientations. The mechanisms influencing the horizontal dispersion for the area studied are likely a combination of small-scale coherent motions and shear predominately forced by the local wind field that is innately variable and episodic.

B. RECOMMENDATIONS FOR FUTURE RESEARCH

The nearshore environment is naturally complex and results from this research did not show equivocally what mechanism or mechanisms were responsible for the horizontal dispersion, therefore additional analysis is recommended for completeness. The data set obtained during SCOPE was robust. The strategy of drifter deployments using triplets of drifters to allow for future use in cluster analysis would provide additional information on vorticity, divergence, shearing and stretching deformations (LaCasce 2008), to aid in a more complete understanding of horizontal mixing. The inner shelf region was relatively shallow at ~ 20 m that may have been a constrain on the flow field that potentially modified the horizontal dispersion results. This boundary influence

was not investigated further during this research, but again would be recommended to investigate in any future research.

This thesis proposed possible mechanisms for influencing the horizontal dispersion for the area of interest, which found the local wind field as the dominant driving mechanism. However, as wind fields are seasonally variant, an understanding of the horizontal mixing regime in the area of interest would be more complete if additional experiments were conducted over different synoptic conditions to ascertain if slacker wind conditions also correlate with the surface current field driving the flow field or if the sub-mesoscale or mesoscale features of the flow start to influence the dispersion to a greater extent under these conditions. Additionally, in conducting another experiment, it may be useful to deploy a combination of surface drifters and deeper drouged drifters to determine the extent of vertical mixing from influences like the wind-drift and Langmuir circulations, to ascertain if this vertical mixing plays a part in the evolution of horizontal dispersion.

THIS PAGE INTENTIONALLY LEFT BLANK

LIST OF REFERENCES

Batchelor, G., 1950: The application of the similarity theory of turbulence to atmospheric diffusion. *Quart. J. Roy. Meteor. Soc.*, **76**, 133–146.

Brown, J., J. MacMahan, A. Reniers, and E. Thornton, 2009: Surf zone diffusivity on a rip-channeled beach. *J. Geophys. Res.,* **114,** C11015, doi:10.1029/2008JC005158.

Consortium for advanced research on transport of hydrocarbon in the environment (CARTHE), cited 2013: Carthe-Overview. [Available online at http://carthe.org/carthe-overview/.]

Davis, R. E., 1991: Observing the general circulation with floats. *Deep Sea Res. Supp.,* **38**, S531-S571.

Drake, P. T., C. A. Edwards, 2009: A linear diffusivity model of near-surface, cross-shore particle dispersion from a numerical simulation of central California's coastal ocean. J. Mar. Res., **67**, 385–409.

Haza, A. C., A. C. Poje, T. M. Özgökmen, and P. Martin, 2008: Relative dispersion from a high-resolution coastal model of the Adriatic Sea. *Ocean Modell.,* **22,** 48–65, doi:10.1016/j.ocemod.2008.01.006.

Haza, A. C., T. M. Özgökmen, A. Griffa, A. Molcard, P.-M. Poulain, G. Peggion, 2010: Transport properties in small-scale coastal flows: relative dispersion from VHF radar measurments in the Gulf of La Spezia. *Ocean Dynam*., **60,** 861–882, doi:10.1007/s10236-010-0301-7.

Hughes, P., 1956: A determination of the relation between wind and sea-surface drift. *Quart. J. Roy. Meteor. Soc.,* **82,** 494–502.

Koszalka, I., J. H. LaCasce and K. A. Orvik, 2009: Relative dispersion in the Nordic Seas, *J. Mar Res*., **67**, 411–433.

LaCasce, J. H., 2008: Statistics from Lagrangian observations. *Prog. Oceanogr.,* **77,** 1–29, doi:10.1016/j.pocean.2008.02.002.

LaCasce, J. H. and A. Bower, 2000: Relative dispersion in the subsurface North Atlantic. *J. Mar Res.,* **58,** 863–894.

LaCasce, J. H. and C. Ohlmann, 2003: Relative dispersion at the surface of the Gulf of Mexico. *J. Mar Res.,* **61,** 285–312.

Leibovich, S., 1983: The form and dynamics of Langmuir circulations. *Ann. Rev. Fluid. Mech.,* **15,** 391–427

Lumpkin, R., and S. Elipot, 2010: Surface drifter pair spreading in the North Atlantic. J. *Geophys. Res.,* **115,** C12017, doi:10.1029/2010JC006338.

McWilliams, J. C. and P. P. Sullivan, 2000: Vertical Mixing by Langmuir Circulations. *Spill Science & Technology Bulletin,* **6(3/4),** 225–237, doi:10.1016/S1353-2561(01)00041-X.

Moroni, M., J. H. Cushman and A. Cenedese, 2002: A 3D-PTV two-projection study of pre-asymptotic dispersion in porous media which are heterogeneous on the bench scale. *Int. J. Eng. Sc.*, **41,** 337–370.

Nerheim, S., A. Stigebrandt, 2006: Horizontal dispersion in the sea caused by recurring changes of the depth of the wind drift. *Geophys. Res. Lett.,* **33,** L12608, doi:10.1029/2006GL026212.

NOAA, Centre for Operational Oceanographic Products and Services (CO-OPS), cited 2014: Meteorological Observations – NOAA Tides & Currents. [Available online at http://tidesandcurrents.noaa.gov/stations.html?type=Water+Levels.]

Ohlmann, J. C., J. H. LaCasce, L. Washburn, A. J. Mariano and B. Emery, 2012: Relative dispersion observations and trajectory modeling in the Santa Barbara Channel. *J Geophys. Res.*, **117,** C05040, doi:10.1029/2011JC007810.

Özgökmen, T.M., A. Griffa, cited 2011. Predictability of Particle Trajectories in the Ocean. [Available online at: http://www.onr.navy.mil /reports/FY10/poozgok1.pdf.]

Poje, C. A., A. C. Haza, T. M. Özgökmen, M. G. Magaldi, Z. D. Garraffo, 2010: Resolution dependent relative dispersion statistics in a hierarchy of ocean models. *Ocean Modell.*, **31,** 36–50, doi:10.1016/j.ocemod.2009.09.002.

Ramseur, J. L., C. L. Hagerty, 2013: *Deepwater Horizon* Oil Spill: Recent Activities and Ongoing Developments. [Available online at: http://www.fas.org/sgp/crs/misc/R42942.pdf.]

Richardson, L., 1926: Atmospheric diffusion shown on a distance-neighbour graph. *Proc. Roy. Soc. London*, **A110,** 709–737.

Romero, L., Y. Uchiyama, J. C. Ohlmann, J. C. Williams and D. A. Siegel, 2013: Simulations of Nearshore Particle-Pair Dispersion in Southern California. J. *Phys Oceanogr.,* **43,** 1862–1879, doi:10.1175/JPO-D-13-011.1.

Schroeder, K., J. Chiggiato, A. C. Haza, A. Griffa, T. M. Özgökmen, P. Zanasca, A. Molcard, M. Borghini, P. M. Poulain, R. Gerin, E. Zambianchi, P. Falco and C. Trees, 2012: Targeted Lagrangian sampling of submesoscale dispersion at a coastal frontal zone. *Geophys. Res. Lett.*, **39,** L11608, doi:10.1029/2012GL051879.

Schroeder, K., A. C. Haza, A. Griffa, T. M. Özgökmen, P. M. Poulain, R. Gerin, G. Peggion, M. Rixen, 2011: Relative dispersion in the Liguro-Provencal basin: From sub-mesoscale to mesoscale. *J. Deep Sea Res.,* **58,** 209–228, doi:10.1016/j.dsr.2010.11.004.

Smith, J. E. (Ed.), 1968: *"Torrey Canyon" Pollution and Marine Life*. Cambridge University Press, 196 pp.

Spydell, M., F, Feddersen, and R. T. Guza, 2007: Observing Surf-Zone Dispersion with Drifters. *J. Phys. Oceanogr.,* **37,** 2920–2939, doi:10.1175/2007JPO3580.1.

Spydell, M., F. Feddersen, and R. T. Guza, 2009: Observations of drifter dispersion in the surfzone: The effect of sheared alongshore currents. *J Geophys. Res.*, **114,** C07028, doi:10.1029/2009JC005328.

Taylor, G., 1921: Diffusion by Continuous Movements. *Proc. London Math. Soc.*, **20**, 196–212.

Wu, J., 1983: Sea-Surface Drift Currents Induced by Wind and Waves. *J. Phys. Oceanogr.,* **13,** 1441–1451.

THIS PAGE INTENTIONALLY LEFT BLANK

INITIAL DISTRIBUTION LIST

1. Defense Technical Information Center
   Ft. Belvoir, Virginia

2. Dudley Knox Library
   Naval Postgraduate School
   Monterey, California